Shear waves Q determination for the upper crust of western and central Slovenia

Shear wave q determination for the upper crust of western and central slovenia

Conference Paper · September 2010

CITATIONS
4

READS
360

5 authors, including:

Vanja Kastelic
National Institute of Geophysics and Volcanology
58 PUBLICATIONS **1,155** CITATIONS
SEE PROFILE

Anastasia A. Kiratzi
Aristotle University of Thessaloniki
172 PUBLICATIONS **4,362** CITATIONS
SEE PROFILE

Christoforos Benetatos
Politecnico di Torino
62 PUBLICATIONS **906** CITATIONS
SEE PROFILE

Mladen Živčić
Slovenian Environment Agency
105 PUBLICATIONS **1,229** CITATIONS
SEE PROFILE

Scientific Annals, School of Geology, Aristotle University of Thessaloniki Proceedings of the XIX CBGA Congress, Thessaloniki, Greece	Special volume 99	377-385	Thessaloniki 2010

SHEAR WAVE Q DETERMINATION FOR THE UPPER CRUST OF WESTERN AND CENTRAL SLOVENIA

Kastelic, V.,[1] Kiratzi, A.,[2] Benetatos, C.,[2] Živčić, M.,[3] and Bajc, J.[4]

[1] *Department of Geology, University of Ljubljana, 1000 Ljubljana, Slovenia*
** now at Istituto Nazionale di Geofisica e Vulcanologia, 00143 Roma, Italy; vanja.kastelic@ingv.it*
[2] *Department of Geophysics, Aristotle University of Thessaloniki, 54124, Thessaloniki, Greece; kiratzi@geo.auth.gr*
[3] *Environmental and Spatial Planning Agency of the Republic of Slovenia, Seismology and Geology Office, Dunajska 47/VII, 1000 Ljubljana, Slovenia; mladen.zivcic@gov.si*
[4] *Faculty of Education, University of Ljubljana, Kardeljeva ploščad 16, 1000 Ljubljana, Slovenia; Jure.Bajc@pef.uni-lj.si*

Abstract: We have estimated the quality factor, Q_β for shear-waves for western and central Slovenia for five frequency bands centred at 0.8 Hz, 1.5 Hz, 3.0 Hz, 6.0 Hz and 12.0 Hz. We used 150 high quality broadband waveforms, from 15 shallow (depth $\leq$ 8km) aftershocks of the 2004 (Mw 5.2) Krn Mountain earthquake sequence in NW Slovenia. Magnitudes (M_L) range from 2.5 to 3.5 and epicentral distances from 16 to 138km. Our results show that Q_β varies with frequency f according to the power law $Q_\beta = 83 f^{0.80}$ or $Q_\beta^{-1} = 0.012 f^{-0.80}$. Comparing our results to those previously obtained for the region of Friuli-Venezia-Giulia in the Southern Alps, both show high values of seismic wave attenuation that is typical of seismogenic active regions and among all sets of data we can observe a good agreement.

Keywords: attenuation; S-waves; *Q* factor; Slovenia; Southern Alps

1. Introduction

Seismic waves attenuate – decrease in amplitude – as they propagate. A cause for such behaviour is the reflection and transmission of seismic waves at discrete discontinuities. In addition, geometric spreading, scattering, multipathing and anelasticity are processes that can reduce wave amplitudes as well. The first three are elastic processes, whereas anelasticity (or else intrinsic attenuation) refers to the reduction of seismic wave amplitudes due to conversion of seismic energy to heat. Attenuation of seismic waves is usually expressed in terms of the dimensionless quality factor Q (Q=2πE/ΔE) or Q^{-1} with ΔE representing the dissipated energy per cycle. Large energy loss means low Q and vice versa, i.e., Q is inversely proportional to the attenuation values.

We chose to study the attenuation of S-waves based on fact that S-waves compared to the P-waves are more destructive. The amplitudes of shear waves are about five times larger compared to the amplitudes of longitudinal waves and their periods are longer by at least a factor of $\sqrt{3}$. These facts arise from differences in wave propagation velocities and the related differences in the corner frequencies of the P - and S – wave source spectra. Thus, the study of the attenuation of shear waves has important engineering implications. Attenuation of direct S-waves (Aki, 1980; Rautian and Khalturin, 1978) contains the combined effect of intrinsic loss and scattering. Attenuation as inferred from the decay rate of coda (Aki and Chouet, 1975; Rautian and Khalturin, 1978) is also the combined effect of scattering and intrinsic attenuation.

Within this study we determined the quality factor, Q_β for shear-waves for the area of western and central Slovenia, using high-quality digital records from the stronger aftershocks of the 2004 Krn Mountain earthquake sequence in NW Slovenia. We estimate Q_β for five frequency bands centred at 0.8 Hz, 1.5 Hz, 3.0 Hz, 6.0 Hz and 12.0 Hz and we mainly follow the procedure described in Polatidis et al. (2003).

2. Regional seismotectonic setting

The studied region (Fig. 1) belongs to two regional structural units. The western and north-western

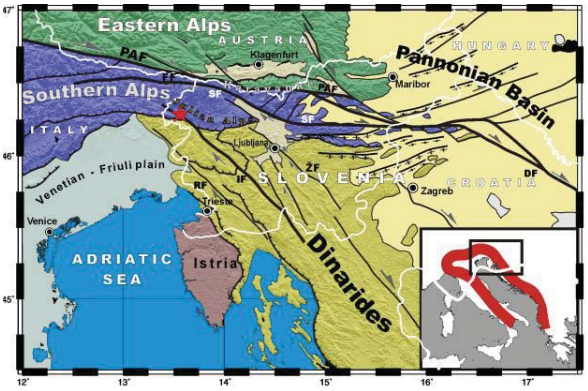

Fig. 1. Regional tectonic framework of Slovenia and neighbouring regions. PAF (Periadriatic fault), FF (Fella fault), SF (Sava fault), SAF (South Alpine thrust front), IF (Idrija fault), RF (Raša Fault), ŽF (Žužemberk Fault), DF (Drava Fault). The thick line in the inset represents a rough position of the Adria microplate. The studied area is shown in the rectangle. The asterisk shows the location of the 2004 Krn mountain sequence, near Julian Alps, lying in the interaction between Southern Alps with E-W trending major tectonic features and Dinarides with NW-SE prevailing structures.

sectors belong to the unit of Southern Alps, while the central and southern parts lie in the structural unit of the Dinarides. The most prominent structures in the unit of Southern Alps are the thrust and reverse faults, trending in an E-W direction with an accompanying N-S oriented shortening. In NW Slovenia, these E-W striking faults interact with NW–SE trending faults that belong to the Dinarides and which display dextral strike-slip kinematics. Two moderate size earthquakes with Mw = 5.6 (Bajc et al., 2001) and Mw = 5.2 (Živčić et al., 2006), occurred in 1998 and 2004, respectively, along a NW-SE trending fault and both main shocks displayed strike-slip kinematics (Kastelic et al., 2008; Bajc et al., 2001; Ganas et al., 2008). The epicentral area of these earthquakes, and especially of the 2004 event which is located more to the NE, lies in the area of interaction between E-W and NW-SE striking faults. This is evident also from the focal mechanisms of aftershocks of the 2004 event that exhibit thrust fault plane solutions, showing N-S shortening on E-W striking faults. Both main shocks and the aftershocks occurred in the shallow parts of the crust with hypocenters not exceeding 8 km in depth, while a number of aftershocks occurred at very shallow depths between 2 and 3 km (Bajc et al., 2001; Kastelic et al., 2006). According to well (Placer et al., 2000) and geophysical data (Behm et al., 2007) the lithology at these depths corresponds to limestone, in the first few kilometres below surface, and to magmatic rocks in greater than 6 km depths. The geological units at the surface display multiple tectonic phases and the density of faults and other structures is high. These faults act as heterogeneities within the crust, which affect the nature of wave propagation.

Previous work related to the attenuation of seismic waves in this part of Southern Alps and Dinarides, is limited and the published work mainly refers to northern Italy, specifically to the region of Friuli-Venezia-Giulia. Console and Rovelli (1981) estimated $Q(f) = 80f^{1.1}$ for the frequency range of 0.1–10 Hz for the Friuli region using strong motion accelerograms at distances up to 200 km, from the 1976 Friuli earthquake sequence. Castro et al. (1996) computed the relation of $Q(f) = 20.4f^{1.1}$ for S waves attenuation in the frequency range 0.4 to 25 Hz, using earthquake data from the same sequence. Govoni et al. (1996) used coda waves of local moderate size earthquakes in the frequency band between 1 to 25 Hz, to obtain $Q(f) = 79f^{0.96}$. For an area of 200 × 200 km extending from Friuli-Venezia Giulia towards Slovenia, Malagnini et al. (2002) in the range of 0.5 to 14 Hz, using ground velocity time-histories from distances 20 to 200 km, obtained a regional propagation model described as $Q(f) = 260f^{0.55}$. For the central part of Slovenia Q values have been determined for P waves using local earthquake recordings. Estimations were done for different time intervals in the frequency bands of 1 to 21 Hz and computed values for lapse time interval of 25 – 45 s give relation of $Q = 123f^{0.69}$ (Ravnik and Živčić, 2000).

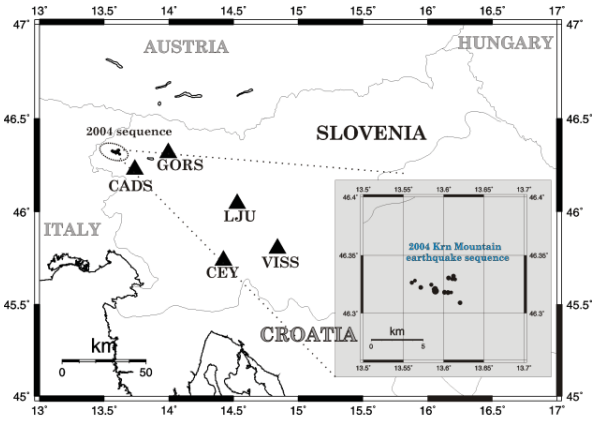

Fig. 2. Geometry of the permanent seismic stations (black triangles) operated by to the Environmental of the Republic of Slovenia, Seismology and Geology Office. The inset depicts the spatial distribution of the 15 stronger aftershocks of the Krn Mountain 2004 earthquake sequence, whose waveforms were analysed in this study.

3. Data

We retrieved the broadband waveforms from the 15 stronger aftershocks of the 2004 Krn Mountain earthquake sequence (Table 1), and we compiled a set of 150 waveforms, in total, from the two horizontal components. The data come from the database of the Seismology office of the Environmental Agency of the Republic of Slovenia, part of the dataset of the permanent network of the Seismic network of the Republic of Slovenia. The equipment of permanent stations consisted of broadband 3-component Guralp CMG-40T seismometers and Quanterra Q730 acquisition unit (Sinčič et al., 2006). The geometry of the station network (Fig. 2) samples parts of western and central Slovenia. Epicentral distances range from 16 to 138 km, M_L values range from 2.5 to 3.5 and depths of aftershocks do not exceed the upper 8 km of the crust. Due to the location of the sequence and the geometry of the network, records from distances in the range 50 to 80 km (Fig. 3) were not available.

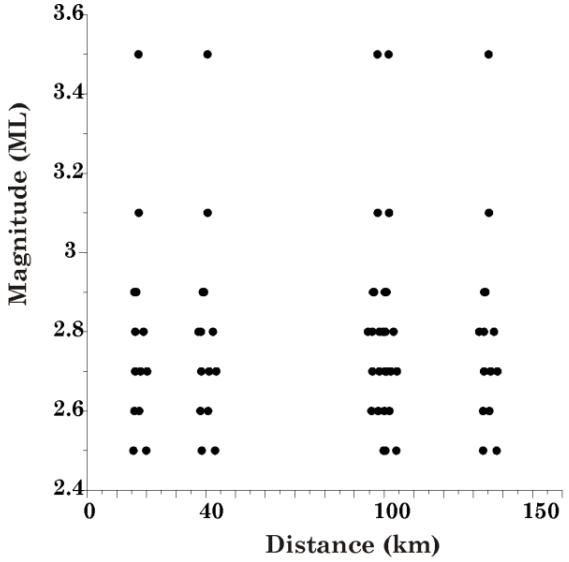

Fig. 3. Distribution of data in magnitude and distance. It is evident that due to the location of the 2004 Krn earthquake sequence and the geometry of the network we have gaps in our distance sampling. We managed to resolve this by averaging the amplitudes over certain distance ranges (see text for details).

We checked the quality of each record based on the signal/noise ratio, by taking the noise spectrum from a time window before the P arrival and the same window over for S-wave (e.g. fig. 4). All records have signals at least a factor of 2 over the noise for a given *fc*. The velocity records from the N-S (HHN) and E-W (HHE) components were baseline corrected, to remove long-period biases, by subtracting the mean and the effect of the instrument response was removed. The records were then band-pass filtered using a Butterworth filter in the frequency range of 0.1 to 20 Hz. Initially, we selected the S-wave time window long enough to include the S-wave train (fig. 5). We applied a 10% cosine taper to both ends of the data and then the Fourier transform was calculated. Then we calculated the corner frequency, f_c using equation (1) of Andrews (1986):

Table 1. Parameters of the 15 stronger aftershocks of the Krn Mountain 2004 earthquake sequence the broadband records of which were analysed in this study.

No.	Date	Time	Latitude	Longitude	Depth	M_L
	YYYY-MM-DD	HHMM	(^{O}N)	(^{O}E)	(km)	
1	2004-07-12	1626	46.3321	13.6122	3.33	2.8
2	2004-07-12	2025	46.3208	13.5877	3.66	2.6
3	2004-07-13	0552	46.3179	13.6054	5.00	2.9
4	2004-07-13	1532	46.3181	13.6011	4.12	2.9
5	2004-07-14	0437	46.3192	13.5898	3.63	3.5
6	2004-07-14	1226	46.3293	13.6141	2.63	2.6
7	2004-07-14	1538	46.3180	13.6093	4.77	2.5
8	2004-07-15	1858	46.3295	13.6109	2.97	2.7
9	2004-07-17	1918	46.3304	13.6061	3.24	2.9
10	2004-07-21	0950	46.3247	13.5846	3.69	2.7
11	2004-07-23	1352	46.3223	13.5716	3.63	2.8
12	2004-08-01	0011	46.3282	13.5644	2.83	2.5
13	2004-08-03	0923	46.3264	13.5604	2.76	2.7
14	2004-08-18	1424	46.3211	13.5893	3.63	3.1
15	2004-11-06	1709	46.3091	13.6203	4.12	2.8

$$f_c = \frac{1}{2\pi}\sqrt{\frac{2\int_0^{+\infty} V^2(f)df}{2\int_0^{+\infty} D^2(f)df}} \qquad (1)$$

where $V^2(f)$ and $D^2(f) = V^2(f)/(2\pi f^2)$ refer to the squared velocity and to the squared displacement power spectra, respectively, calculated for the S-wave train considered. This initial value of f_c was then used to calculate the signal duration, T_d of the S-wave strong ground motion using the formula of Hermann (1985):

$$T_d = \frac{1}{f_c} + 0.05R \qquad (2)$$

where R is the epicentral distance in km. The ground motion duration thus obtained was used to select an S-wave time window equal to this duration (as obtained from eq. 2) and the Fourier transform was again calculated. The calculated S-wave durations were in good agreement with those visually selected from the original records. In this way the S-wave time windows analysed were between 1.8 and 7.5 s and the corner frequencies calculated were between 1.8 and 7.5 Hz. Averages of the S-wave amplitude were taken over one octave frequency bands centred at 0.8, 1.5, 3.0, 6.0 and 12.0 Hz.

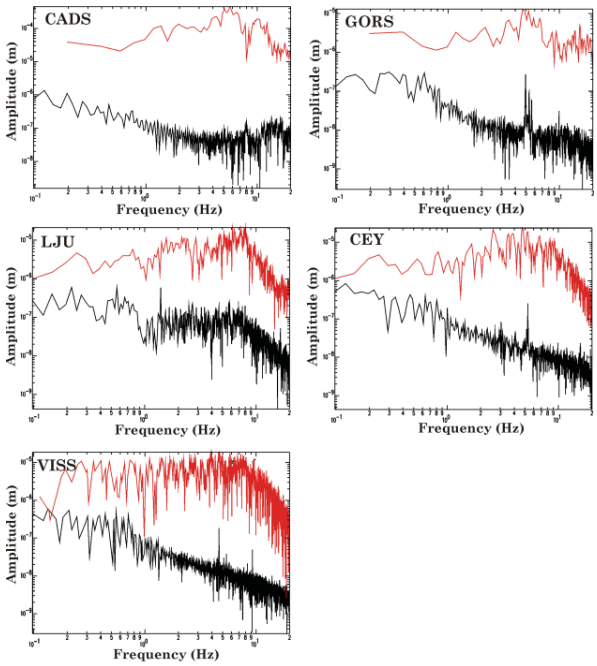

Fig. 4. Example of earthquake spectra for signal (top trace, in red) and noise (bottom trace, in black) for frequency bands between 0.01 and 20 Hz. This analysis was performed for all aftershocks and for all records. For each record, we checked the frequency ranges for which the signal/noise ratio was higher than 2.

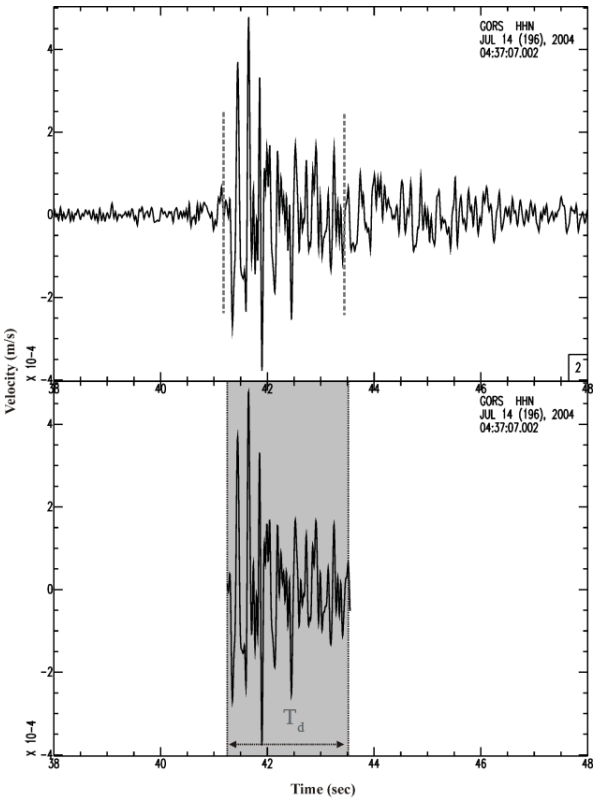

Fig. 5. Example of the procedure followed to calculate the duration T_d for the S-wave train, which was included in the spectral analysis. The top record depicts the initially selected time window we used for corner frequency determination. For T_d we used equation of $T_d = 1/f_C + 0.05R$ to calculate the corresponding time for the S-wave train at the epicentral distance of R is the epicentral distance for used event and seismic station is 40.55 km km that gave the value $T_d = 2.3$ s (lower image). Using this duration time we again selected the appropriate time window to calculate its Fourier transform.

4. Method of analysis

We used empirical functions that describe the observed trends of the spectral amplitude decay with distance using a nonparametric method (Anderson and Quaas, 1988; Castro *et al.,* 1990, 1999, 2002; Anderson and Lei 1994, see also the application in Polatidis *et al.,* 2003). The dependence of the S-wave spectral amplitudes U on hypocentral distance R for a given frequency f was modeled as:

$$U_i(f,R) = S_i(f)\cdot A(f,R) \qquad (3)$$

where $U_i(f, R)$ is the observed spectral amplitude of

event i, $A(f, R)$ is the empirically determined attenuation function that describes the distance decay trend, and $S_i(f)$ is a scalar (one for each earthquake i at frequency f) that depends on the size of the earthquake. $A(f, R)$ contains the effects of both the geometrical spreading and the quality factor Q but is not limited to a particular functional form. The attenuation function *A(f, R)* using a homogeneous attenuation model, is further parameterized as:

$$A(f,R) = R^{-n} \exp(-\frac{\pi f R}{Q_\beta(f)\beta}) \qquad (4)$$

where f is the frequency, β is the velocity of S-waves taken equal to 3.4 km/sec and R^{-n} is the geometrical spreading function. The attenuation functions, *A(f, R)* were obtained empirically in the frequency band of 0.6 to 16 Hz by fitting the spectral amplitude decay of the records. Using (3) equation (4) becomes:

$$U_i(f,R) = S_i(f) R^{-n} \exp(-\frac{\pi f R}{Q_\beta(f)\beta}) \qquad (5)$$

and taking the logarithm of (5) and rearranging we get:

$$\log U_i(f,R) + n \log R = \log S_i(f) - \pi \log(e) \frac{f}{\beta Q_\beta(f)} R \quad (6)$$

For the distances used here ($R \leq 138$ km) we assume a decay rate of $1/R$ (n=1), which implies body wave propagation and spherical geometry. In fact, all epicentral distances are within 100 km, only one of the stations used exceeded 100 km, but was still in the range for direct S-waves arrivals. Correcting the observed spectral amplitudes for the effects of geometrical spreading and plotting $\{\log U_i(f,R) + n \log R\}$ versus R, for each aftershock and frequency range, the value of $-\pi \log(e) \frac{f}{\beta Q_\beta(f)}$ corresponds to the slope b of the line of the least squares fit. To calculate Q_β values, for each designated centre frequency, f we simply used the form: $Q_\beta(f) = \frac{-\pi \log(e) f}{b\beta}$.

5. Results

We show an example (Fig. 6) of the procedure followed to estimate $Q_\beta(f)$ for a single event (No. 9 in Table 1). As described previously Q_β was determined for the five centre frequencies as a relation between logarithmic values of amplitude and epicentral distance, R. The slope of the least squares' fit, the Q_β values and correlation coefficient of the regression, are also included in the plots. The frequency dependence of Q_β, for this specific event, is approximated as: $Q_\beta(f) = 49 f^{0.75}$.

Table 2 lists the $Q_\beta(f)$ values for all the 15 events used in this study, for each centre frequency, and for each horizontal component, separately. It also lists the mean Q_β values and their frequency dependence, for each component separately and for both. One observation from the mean results listed in Table 2 is the large variation of Q_β values for individual events, reflected in the standard deviation of the mean. This was also observed in similar studies (Hatzidimitriou, 1995; Polatidis *et al.,* 2003; Baskoutas et al., 2004) for other regions and was mainly attributed to the fact that the amplitude decrease due to geometrical spreading can be more than R^{-1}.

At a next step we normalized spectral amplitudes to a reference earthquake of magnitude M_L=2.8 (the maximum likelihood estimate of the data distribution) and we have recalculated Q values using the normalized data set (fig. 7). To improve the quality of the regression we have included the data from both components and we have also calculated average spectral amplitudes for average distances for six distance ranges, which we determined based on the distribution of data in distance (see also fig. 3). More specifically for the distance ranges 15 to 20km, 21 to 39km, 40 to 44km, 45 to 100km, 101 to 104km and 105 to 138km we have calculated average spectral amplitudes and average distance. These average values (standard deviation of distances ~1.25 km and ~0.24 in spectral amplitudes) were used in the regression (Fig. 8), constraining the regression better, improving the fit and we chose to adopt these results as our preferred fits. The results $Q_\beta(f) = 83 f^{0.80}$ show strong frequency dependence (included in Table 3).

6. Conclusions

Data from 150 broadband waveforms belonging to 15 aftershocks of the 2004 Krn Mountain earthquake sequence were analysed to study the frequency dependence of direct S-wave attenuation in western and central Slovenia. The epicentral distances of the events range from 16 to 138 km and

Table 2. Q_β values of all earthquakes for the five centre frequencies and correlation coefficient, r of the least square fit, are shown separately for both horizontal channel components. Values 0 for r and Q_β values in parenthesis represent low corellation, thus data were excluded from the summation to obtain the mean Q_β for each centre frequency. Blank lines in two cases for the HHN channel represent poor quality data that were not used in the analysis.

Date	ML	0.6 - 1.0 Hz	r	1.0 - 2.0 Hz	r	2.0 - 4.0 Hz	r	4.0 - 8.0 Hz	r	8.0 - 16.0 Hz	r
YYYY-MM-DD		Centre frequency		Centre frequency		Centre frequency		Centre frequency		Centre frequency	
		0.8 Hz		**1.5 Hz**		**3.0 Hz**		**6.0 Hz**		**12.0 Hz**	
HHE channel		Q_β		Q_β		Q_β		Q_β		Q_β	
2004-07-12	2.8	27	0.91	75	0.82	135	0.90	194	0.95	326	0.96
2004-07-12	2.6	39	0.63	84	0.82	169	0.97	222	0.85	335	0.93
2004-07-13	2.9	42	0.59	(101)	0	(176)	0	204	0.79	446	0.90
2004-07-13	2.9	40	0.65	81	0.94	122	0.92	280	1.00	370	0.97
2004-07-14	3.5	45	0.63	74	0.81	124	0.98	209	0.87	381	0.94
2004-07-14	2.6	26	0.76	66	0.71	113	0.81	177	0.92	304	0.97
2004-07-14	2.5	56	0.48	(99)	0	(177)	0	187	0.81	330	0.84
2004-07-15	2.7	29	0.94	74	0.83	122	0.92	142	0.97	325	0.91
2004-07-17	2.9	38	0.91	75	0.93	110	0.91	171	0.90	325	0.89
2004-07-21	2.7	40	0.64	83	0.71	152	0.92	271	0.82	363	0.94
2004-07-23	2.8	30	0.64	86	0.54	143	0.52	207	0.80	357	0.88
2004-08-01	2.5	53	0.85	90	0.82	316	0.54	317	0.86	417	0.97
2004-08-03	2.7	37	0.90	73	0.91	208	0.94	231	0.91	410	0.96
2004-08-18	3.1	34	0.70	76	0.70	167	0.96	196	0.88	354	0.93
2004-11-06	2.8	52	0.55	123	0.70	156	0.98	252	0.89	402	0.91
HHE Average Q_β		***$Q_\beta = 39 \pm 9$***		***$Q_\beta = 82 \pm 14$***		***$Q_\beta = 157 \pm 55$***		***$Q_\beta = 217 \pm 46$***		***$Q_\beta = 363 \pm 41$***	
HHE Power fit						***$Q_\beta = 54 f^{0.80}$***					
HHN channel		Q_β		Q_β		Q_β		Q_β		Q_β	
2004-07-12	2.8	30	0.96	60	0.76	114	0.87	195	0.88	298	0.94
2004-07-12	2.6	57	0.74	116	0.66	218	0.93	301	0.80	402	0.95
2004-07-13	2.9	n/a	n/a	n/a	n/a	n/a	n/a	n/a	n/a	n/a	n/a
2004-07-13	2.9	36	0.70	97	0.77	191	0.84	227	0.97	370	0.97
2004-07-14	3.5	99	0.78	104	0.85	197	0.96	282	0.92	429	0.99
2004-07-14	2.6	45	0.72	68	0.66	126	0.77	217	0.88	345	0.93
2004-07-14	2.5	n/a	n/a	n/a	n/a	n/a	n/a	n/a	n/a	n/a	n/a
2004-07-15	2.7	37	0.93	62	0.73	93	0.86	208	0.81	334	0.89
2004-07-17	2.9	32	0.95	56	0.75	93	0.62	181	0.91	318	0.91
2004-07-21	2.7	53	0.69	(128)	0	234	0.72	285	0.84	391	0.95
2004-07-23	2.8	45	0.67	71	0.73	178	0.90	352	0.81	468	0.97
2004-08-01	2.5	31	0.62	113	0.53	191	0.86	376	0.66	439	0.98
2004-08-03	2.7	29	0.64	89	0.66	165	0.87	238	0.84	403	0.90
2004-08-18	3.1	54	0.66	95	0.59	199	0.88	272	0.78	372	0.94
2004-11-06	2.8	48	0.72	(203)	0	200	0.67	307	0.73	426	0.95
HHN Average Q_β		***$Q_\beta = 46 \pm 19$***		***$Q_\beta = 85 \pm 22$***		***$Q_\beta = 161 \pm 46$***		***$Q_\beta = 265 \pm 60$***		***$Q_\beta = 384 \pm 50$***	
HHN Power fit						***$Q_\beta = 60 f^{0.79}$***					
Both components Average Q_β		***$Q_\beta = 42 \pm 14$***		***$Q_\beta = 83 \pm 18$***		***$Q_\beta = 158 \pm 50$***		***$Q_\beta = 239 \pm 57$***		***$Q_\beta = 373 \pm 46$***	
Both components Power fit						***$Q_\beta = 57 f^{0.80}$***					

the M_L magnitudes from 2.5 to 3.5. The focal depths of the events are confined within the upper 5 km of the crust. The region of study geodynamic-cally lies in the transition between the units of Southern Alps and Dinarides. Julian Alps and Friuli region belong to the part of the Alpine orogen with the highest seismic activity. This is the region of occurrence of the strong 1976 M_W= 6.4 (Barbano et al., 1985; Slejko et al., 1999; Pondrelli et al., 2001), and of the moderate magnitude earthquake sequence of the 1998 M_w= 5.6 (Bajc et al., 2001) and of the 2002 M_W= 4.9 (Bressan et al., 2007) and the 2004 M_W= 5.2 (Živčić et al., 2006) events.

In the frequency band of 0.6 to 16 Hz, and for distances from 16 up to 138 km, the frequency dependence of Q_β can be approximated as $Q_\beta = 83 f^{0.80}$ or $Q_\beta^{-1} = 0.012 f^{-0.80}$. We obtained values Q_β separatelly for HHN and HHE channels with calculated values of $Q_{\beta\mathrm{HHE}} = 54 f^{0.80}$ and

Table 3. $Q_{\beta\ normalized}$ are the $Q_\beta(f)$ values calculated when all spectral amplitudes have been normalized to a reference ML=2.8 earthquake.

f (Hz)	$Q_{\beta\ normalized}$ HHE component	$Q_{\beta\ normalized}$ HHN component	$Q_{\beta\ normalized}$ Both components
0.8	58	64	60
1.5	122	123	124
3	231	232	232
6	356	340	342
12	543	564	546
	$Q_\beta = 81f^{0.81}$	$Q_\beta = 85f^{0.79}$	$Q_\beta = 83f^{0.80}$

$Q_{\beta HHN} = 57f^{0.80}$. The small difference between the HHE and HHN spectral decay is within the statistical uncertainties of the estimates, suggesting that Q anisotropy is negligible. However, only considering high frequencies bands (f = 4-8 and f = 8-16 Hz), we observed values of $Q_{\beta\ HHN}$ which are significantly above the values for $Q_{\beta HHE}$. Comparing our results to those previously obtained (Fig. 8) for the region of Friuli-Venezia-Giulia in the Southern Alps we can observe a good agreement. The only relation directly applicable to Slovenia (No. 2 in Fig. 8) shows the attenuation of P-waves and compares well with our relation (No. 3 in Fig. 8) which describes the faster attenuation of S-waves in Slo-

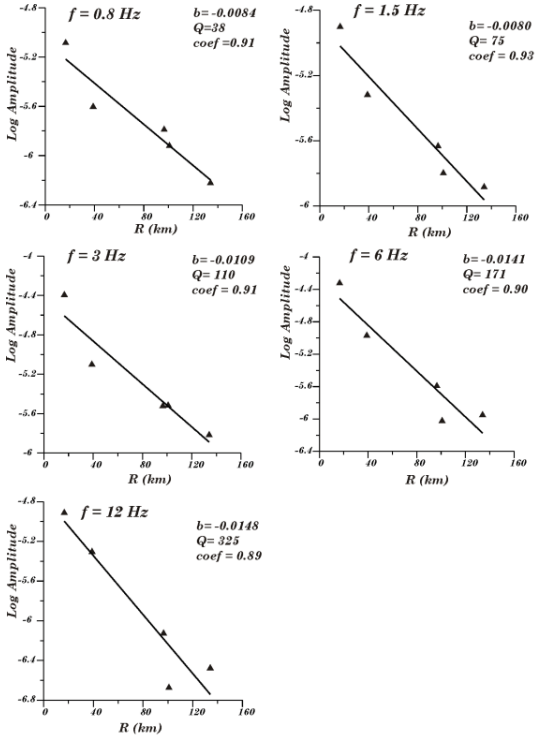

Fig. 6. Example of Q_β determination for the five centre frequencies selected for earthquake No 9 (Table 1). Values of the slope, b, and correlation coefficient, $coef$, of the linear least squares fit and the computed Q_β values are also included in the plots.

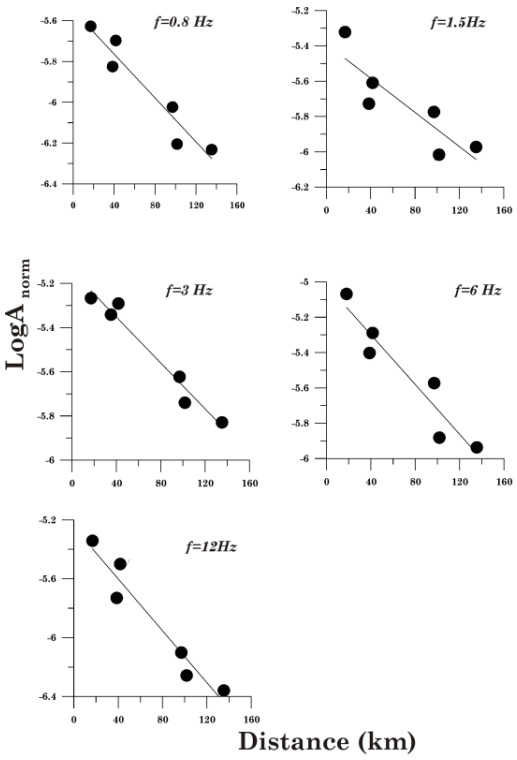

Fig. 7. Variation of spectral amplitudes with distance for each centre frequency. All spectral amplitudes have been normalized to a reference magnitude ML=2.8. Amplitudes were averaged for certain distance ranges in order to better constrain the regression. In this plot, we have used all data from both horizontal components.

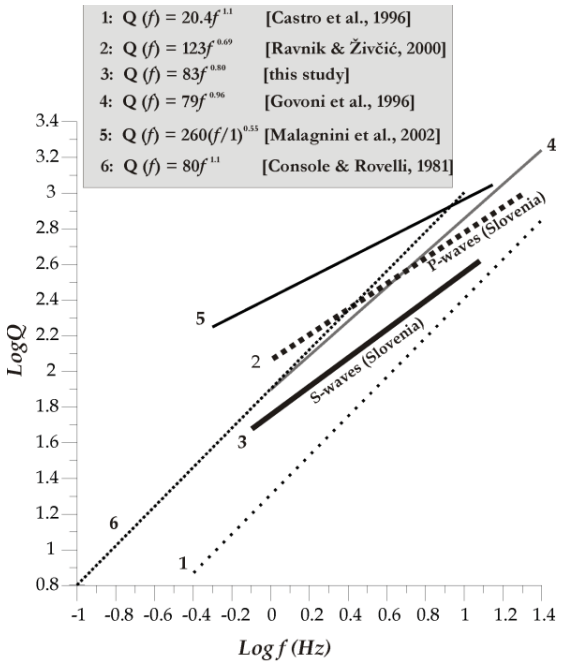

Fig. 8. Comparison of attenuation relations – mainly for the region of Friuli-Venezia Giulia and our results for S-wave attenuation in Slovenia (No. 3). Note that the only relation applicable to Slovenia describes P-wave attenuation (No. 2). Our results indicate faster attenuation of S-waves in Slovenia compared to the P-wave attenuation.

venia. Our results are comparable to worldwide Q_β^{-1} values for the lithosphere (Sato et al., 2002), which predict that Q_β^{-1} is of the order of 10^{-2} at 1 Hz and decreases to the order of 10^{-3} at 20 Hz. As coda waves are composed of *S* waves (Aki, 1992) and that the attenuation mechanism of coda waves is similar to that of the direct *S* waves (Aki, 1980), at a first approximation, we may assume that our results describe coda wave attenuation in western and central Slovenia, as well.

Acknowledgements

AK and CB acknowledge support from General Secretariat of Research and Technology of Greece. VK acknowledges financial support of Ad futura, scientific-educational foundation of Republic of Slovenia, contract 2006/523-24.

References

Aki K., 1980. Attenuation of shear-waves in the lithosphere for frequencies from 0.05 to 25 Hz. *Phys. Earth and Planet. Inter.* 21, 50–60.

Aki K., 1992. Scattering conversions *P* to *S* versus *S* to *P*, *Bull. Seism. Soc. Am.* 82, 1969-1972.

Aki K. and Chouet B., 1975. Origin of coda waves: source, attenuation and scattering effects. *J. Geophys. Res.,* 80, 3322–3342.

Anderson J., and Lei Y., 1994. Nonparametric description of peak acceleration as a function of magnitude, distance and site in Guerrero Mexico. *Bull. Seismol. Soc. Am.* 84, 1003– 1017.

Anderson J., and Quaas R., 1988. The Mexico earthquake of September 19, 1985, effect of magnitude on the character of strong ground motion: an example from the Guerrero Mexico strong motion network. *Earthq. Spectra* 4, 635–646.

Andrews D.J., 1986. Objective determination of source parameters and similarity of earthquakes of different size. In: Proceedings of the 5th Maurice Ewing Symposium on Earthquake Source Mechanics, Das, S., Boatwright, J., Scholz, C. (Eds.), American Geophysical Union, Washington, DC, pp. 259– 268.

Bajc J., Aoudia A., Sarao A. and Suhadolc P., 2001. The Bovec – Krn mountain (Slovenia) earthquake sequence. *Geophysical Research Letters*, Vol. 28, No. 9, 1839 – 1842.

Barbano M.S., Kind R. and Zonno G., 1985. Focal parameters of some Friuli earthquakes (1976–1979) using complete theoretical seismograms. *J. Geophys. Res.* 58, 175–182.

Baskoutas I., Herraiz M., Pérez A.C., Kalogeras I., Panopoulou G., Sachpazi M. and Papadopoulos G., 2004. Mapping of coda attenuation at the extent of the national seismological network of Greece. *Bulletin of the Geological Society of Greece,* vol. XXXVI, 232-242.

Behm M., Brückl E., Chawatal W. and Thybo F., 2007. Application of stacking and inversion techniques to three-dimensional wide-angle reflection and refraction seismic data of the Eastern Alps. *Geophys. J. Int.* 170, 1, 275-298, doi: 10.1111/j.1365-246X.2007.03393.x

Bressan G., Kravanja S. and Franseschina G., 2007. Source parameters and stress release of seismic sequences occured in the Friuli/Veneyia Giulia region (Northeastern Italy) and Western Slovenia. *Physics of the Earth and Planetary Interiors* 160, 192-214.

Castro R.R., Anderson J.G. and Singh S.K., 1990. Site response, attenuation and source spectra of S waves along the Guerrero Mexico, subduction zone. *Bull. Seismol. Soc. Am.* 80, 1481–1503.

Castro R.R., Pacor F., Sala A. and Petrungaro C., 1996. S-wave attenuation and site effects in the region of Friuli, Italy. *J. Geophys. Res.* 101, 22,355–22,369.

Castro R.R., Monachesi G., Mucciareli M., Trojani L. and Pacor F., 1999. P- and S- wave attenuation in the region of Marche, Italy. *Tectonophysics* 302 (1), 123– 132.

Castro R.R., Monachesi G., Trojani L., Mucciareli M. and Frapiccini M., 2002. An attenuation study using earthquakes from the 1997 Umbria– Marche sequence. *J. Seismol.* 6, 43–59.

Console R. and Rovelli A., 1981. Attenuation parameters for Friuli region from strong-motion accelerograms spectra. *Bull. Seism. Soc. Am.* 71, 1981–1991.

Ganas A., Gosar A. and Drakatos G., 2008. Static stress changes due to the 1998 and 2004 Krn Mountain (Slovenia) earthquakes and implications for future seismicity. *Nat. Hazards Earth Syst. Sci.,* 8, 59-66.

Govoni A., Bragato P.L. and Bressan G., 1996. Coda *Qc* evaluation using local seismic events in the Friuli area. *Atti del 15◦ Convegno G.N.G.T.S.*, Roma Italy, pp. 389–392.

Hatzidimitriou P.M., 1995. S-wave attenuation in the crust in Northern Greece, *Bull. Seism. Soc. Am.* 85, 1381–1387.

Herrmann R., 1985. An extension of random vibration theory estimates of strong ground motions to large distances. *Bull. Seismol. Soc. Am.* 75, 1447–1453.

Kastelic V., Živčić M., Pahor J., Gosar A., 2006. Seismotectonic characteristics of the 2004 earthquake in Krn Mountains. *Potresi v letu* 2004, EARS, 78-87.

Kastelic V., Vrabec M., Cunningham D. and. Gosar A., 2008. Neo-Alpine structural evolution and present-day tectonic activity of the eastern Southern Alps: The case of the Ravne Fault, NW Slovenia. *J. Struct. Geol.,* 30, 963–975. doi:10.1016/j.jsg.2008. 03.009.

Malagnini L., Akinci A., Herrmann R.B., Pino N.A., Scognamiglio L., 2002. Characteristics of the ground motion in Northeastern Italy. *Bull. Seism. Soc. Am.* 92, 2186–2204.

Placer L., Rajver D., Trajanova M., Ogorelec B., Skaberne D., Mlakar I., 2000. Borehole Ce-2/95 at Cerkno at the boundary between the Southern Alps and the External Dinarides (Slovenia). *Geologija* 43/2, 251-266.

Polatidis A., Kiratzi A., Hatzidimitriou P. and Margaris B., 2003. Attenuation of shear-waves in the back-arc region of the Hellenic arc for frequencies from 0.6 to 16 Hz. *Tectonophysics,* 367, 29-40.

Pondrelli S., Ekström G., Morelli A., 2001. Seismotectonic re-evaluation of the 1976 Friuli, Italy, seismic sequence. *Journal of Seismology*, 5, 73-83.

Rautian T.G., Khalturin V.I., 1978. The use of coda for determination of the earthquake source spectrum. *Bull. Seismol. Soc. Am.* 68, 923–948.

Ravnik J., Živčić M., 2000. Coda *Q* from earthquakes in central Slovenia. Potresi v letu 2000, (EARS), 95-104.

Sato H., Fehler M. and Wu R.-S., 2002. Scattering and attenuation of seismic waves in the lithosphere. In: Lee, W.H.K., Kanamori, H., Jennings, P.C., Kisslinger, C. (Eds.), International Handbook of Earthquake and Engineering Seismology. Academic Press, New York. Chap. 13.

Sinčič P., Vidrih R., Gostinčar M., Tasič I., Živčić M., 2006: Seismic network in Slovenia 2004. *Potresi v letu* 2004, (EARS), 1-15.

Slejko D., Neri G., Orozova I., Renner G. and Wyss M., 1999. Stress field in Friuli (NE Italy) from fault plane solutions of activity following the 1976 main shock. *Bull. Seism. Soc. Am.* 89, 1037–1052.

Živčić M. and Krn-2004 team, 2006. The Krn mountains (Slovenia) MW 5.2 earthquake: data acquisition and preliminary results. *Geophysical Research Abstracts*, 8, 06439.